Optimization of a Low-cost Corona-DBD Plasma Wastewater Treatment System through CCD/RSM with Mechanistic and Efficiency Analysis

Yiting Xiao *, Yang Tian, Yuanhang Zhan, And Jun Zhu *

Posted Date: 11 December 2023

doi: 10.20944/preprints202312.0738.v1

Keywords: Water purification; non-thermal plasma; reactor design; advanced purification systems

Article

Optimization of a Low-Cost Corona-DBD Plasma Wastewater Treatment System through CCD/RSM with Mechanistic and Efficiency Analysis

Yiting Xiao [1,†], Yang Tian [2,†], Yuanhang Zhan [1] and Jun Zhu [1,*]

[1] Biological Engineering, University of Arkansas, Fayetteville, 72701, USA; yx011@uark.edu (Y.X.); yz062@uark.edu (Y.Z.)
[2] Material Science and Engineering Programs, University of Arkansas, Fayetteville, AR 72701, USA; yangtian@uark.edu
* Correspondence: junzhu@uark.edu
† These authors contributed equally to this work.

Abstract: Water pollution, intensified by the release of hard-to-degrade pollutants, poses severe threats to ecosystems, human health, and economic development. The existing advanced oxidation processes often involve high operational costs and may result in secondary pollution, highlighting the necessity for innovative and more sustainable solutions. To address these challenges, our study introduces a cost-effective and eco-friendly corona discharge barrier plasma discharger for wastewater treatment. Through the central composite design/response surface methodology, a high decolorization rate of 98% of methylene blue (MB) within 10 minutes was achieved by optimizing parameters such as pH and voltage. Furthermore, the mechanisms of the generation of reactive oxygen species via this device was discussed in detail and the degradation pathways of MB were described. Moreover, this device is also very energy-efficient, with a low energy density and electrical energy per order of 0.15 watt/mL and 5.79 kWh/m^3/order, respectively. In conclusion, the plasma discharger developed in this study provides a cost-effective and environmentally sustainable solution for dye wastewater treatment. This research contributes significantly to the advancement of sustainable dye wastewater management practices, offering an innovative method that meets both environmental and economic objectives.

Keywords: water purification; non-thermal plasma; reactor design; advanced purification systems

1. Introduction

Water pollution remains one of the most severe environmental challenges of the modern era, with its impact intensified by the release of hard-to-degrade pollutants, posing significant threats to ecosystems, human health, and economic development. Artificial organic dyes, extensively used in textiles and leather industries, are major contributors to water pollution. Currently, the market offers over 10,000 different dyes, with global production exceeding 700,000 metric tons each year, 5% to 10% of which end up in industrial wastewater [1]. A dye concentration range of 10 to 50 mg/L can markedly affect water transparency, disrupt aesthetic qualities, and reduce the solubility of gases in water, thereby influencing the ecological balance of aquatic systems [2]. Moreover, the infiltration of these dyes into ecosystems contributes to water quality degradation and poses enduring environmental and health risks, given their toxicity, resistance to biodegradation, and accumulation in water, soil, and the aquatic food chain. Methyl blue (MB), a cationic dye with a triphenylmethane structure, is prevalent in various industries and medical practices. It is employed for dyeing textiles such as wool and cotton, and in paper production for coloring and coating. In the medical field, MB is used as an antiseptic and diagnostic aid, aiding in tissue staining and visualization during surgical procedures. Despite its utility, MB poses health risks to humans and animals; it is generally safe in therapeutic doses, but overexposure can lead to eye irritation, dry mouth, tachycardia, nausea, vomiting, abdominal pain, diarrhea, visual disturbances, hemolytic anemia, and methemoglobinemia [3]. Moorthy et al. also reported that MB can be categorized as toxic to aquatic organisms according to EU-Directive 93/67/EEC [4]. Consequently, the development of efficient

 doi:10.20944/preprints202312.0738.v1

methods to eliminate MB from industrial wastewater is critical to safeguarding environmental and public health.

Traditional methods for treating dye wastewater, such as coagulation, flocculation, membrane filtration, adsorption, and ion exchange, have demonstrated initial effectiveness in decolorizing wastewater. These methods, however, often entail high capital and recurring costs, making them economically unsustainable for many industries [5,6]. Additionally, they frequently result in the formation of sludge or require the regeneration of adsorbent materials, limiting their broader application. Advanced oxidation processes (AOPs), including techniques like the ozone peroxide advanced oxidation process (O_3-H_2O_2), have emerged as promising alternatives. AOPs work by creating reactive species like hydroxyl free radicals, effectively breaking down water pollutants into carbon dioxide and water through mineralization [7,8]. These processes are particularly good at decomposing stubborn materials and toxic contaminants. However, AOPs often require extensive use of oxidants and other chemicals, raising concerns about secondary pollution and the broader environmental impact [9]. Additionally, they are not always cost-effective due to the need for additional equipment such as ozone generators, hydrogen peroxide storage and injection facilities, and comprehensive monitoring and control systems [10,11]. This need for additional equipment and chemical use has led to ongoing research aimed at developing more cost-effective and efficient methods for the single-step production of reactive oxygen and nitrogen species, with the goal of improving wastewater treatment processes.

In recent years, non-thermal plasma technology has gained significant attention for its ability to degrade complex and stubborn organic compounds. This technology has found extensive applications in environmental clean-up, particularly in the treatment of pollutants that are otherwise difficult to break down using conventional methods [12]. Non-thermal plasma operates efficiently at breaking down a wide range of hazardous substances, making it a versatile tool in tackling environmental challenges. The effectiveness of non-thermal plasma stems from its ability to generate a variety of reactive species that can attack and decompose complex molecular structures found in various pollutants [13]. Its applications extend beyond environmental remediation to include air purification, surface treatment, and even in the medical field for sterilization and therapy. Its efficiency and adaptability have led to its adoption across multiple sectors for sustainable management and treatment of complex pollutants. One major concern with plasma technology, despite its advancements, is its high energy consumption. Additionally, while numerous studies have indicated pH fluctuations during the discharge process due to the formation of various ionic species, there remains a research gap in understanding the effect of initial pH on the degradation of organic pollutants.

To address these issues, this study introduces an innovative wastewater treatment method through the development of an ultra-low-cost corona discharge barrier discharge (cDBD). The central composite design/response surface methodology (CCD/RSM) was employed to investigate the effect of the initial pH and voltage and to optimize the degradation efficiency. This study provides a thorough analysis of the mechanisms driving the generation of reactive oxygen species (ROS) and the breakdown of MB, along with a detailed exploration of the chemical mechanisms by which pH and voltage influence pollutant removal efficiency. These insights can help in achieving a low energy consumption in large-scale operations, thereby improving the sustainability and effectiveness of this treatment method.

2. Materials and Methods

2.1. Experimental setup

A schematic diagram of the cDBD Plasma Micro-Reactor is shown in Figure 1. The reactor's main body was constructed using a 20 mL scintillation vial, with a working volume of 10 mL and an outer diameter of 28 mm. An 18-gauge copper wire served as the live electrode, while a 0.1 mm thick, 0.5-inch-long copper tape was coiled around the glass tube as the ground electrode. The discharge gap between the electrodes was 1 mm. An adjustable 24V DC dual display fixed current power supply

Preprints (www.preprints.org) | NOT PEER-REVIEWED | Posted: 11 December 2023 doi:10.20944/preprints202312.0738.v1

was used to test the optimal voltage range. The amplified voltage that was applied to the reactor varied between 28–33 kV. The working frequency was 0.3 Hz with a 50% duty cycle. and the initial dye concentration was 10 mg/L, and the treatment time was 10 min (working time: 5 min).

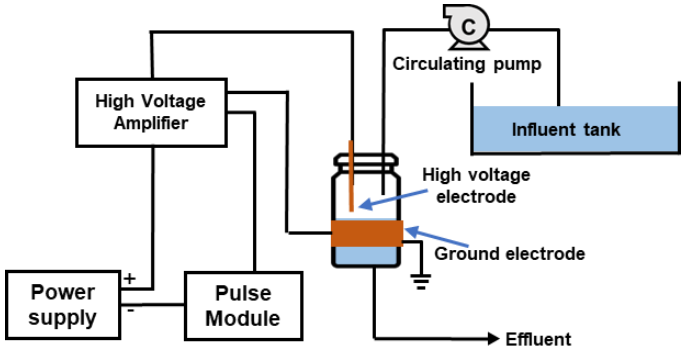

Figure 1. Schematic diagrams of the cDBD reactor.

2.2. Methods and analysis

All chemicals used were analytical grade without any further purification. MB (1% w/v) was purchased from BeanTown Chemical Inc. (Hudson, NH, USA) and was diluted to 10 mg/L. Sulfuric acid (95-98%) and sodium hydroxide (≥97.0%; beads) were purchased from VWR International (Radnor, PA, USA). The pH of the solution was determined using a PHS-25 digital-display pH meter (XL 600, Fisher Scientific, Hampton, NH, USA).

To assess the dye concentration throughout the treatment process, samples were regularly collected and analyzed for absorbance at approximately 664 nm (λ_{max}) using a SpectroVis® Plus Spectrophotometer from Vernier Software & Technology (Beaverton, OR, USA) with a 10 mm plastic cuvette. The breakdown of the dye was quantified based on the decolorization rate, and the decolorization rate of the samples was calculated as:

$$Decolorization \text{ rate } \% = (1 - \frac{C_{ci} - C_{cf}}{C_{ci}}) \times 100\% \quad (1)$$

where, C_{ci} and C_{cf} are the MB concentrations at time t = 0 and treatment time t, respectively.

2.3. Experimental design

In this study, pH of the MB solution and the voltage applied were selected as independent variables to determine their effects on the performance of the plasma discharger, where the decolorization rate was used as the response variable. Each independent variable ranged over five levels between – alpha (α) and + α , 4 to 9 for pH and 28 to 33 kV for voltage. These levels were chosen based on preliminary trials. Experimental design was conducted using the RSM through the CCD in the statistical software Design-Expert (version 13.0.1.0, Stat-Ease Inc, Minneapolis, MN, USA) to generate the experimental runs and determine the optimal combination of these two independent variables to maximize the efficiency for the degradation process according to the experimental results. A total of 13 (2k + 2k + cp, where k is the number of factors and cp is the number of center points) experiments for the two factors with five center points were conducted. **Table 1** shows the independent experimental factors and their levels in the CCD.

Table 1. Factors and their levels for central composite design.

	Code	Coded and actual levels				
Factors	**X_i**	**−1.414 (−α)**	**−1 (Low)**	**0 (Center)**	**1 (High)**	**1.414 (+α)**
Voltage (kV)	X_1	27	28	30.5	33	34
pH	X_2	3.0	4.00	6.5	9	10.0

 doi:10.20944/preprints202312.0738.v1

3. Results and Discussion

3.1. Evaluation of the model fitting and the statistical analysis

Error! Reference source not found. illustrates the design matrix and the outcomes of experiments assessing the effectiveness of MB dye degradation in the microreactor over a treatment period of 10 minutes. Utilizing a Central Composite Design (CCD), the Design-Expert software developed a quadratic model based on the experimental data in Table 2, focusing on two independent variables: voltage (X_1) and pH (X_2). The resulting models demonstrated a proficient capability in predicting the dye decomposition rate. Additionally, Analysis of Variance (ANOVA) was employed to evaluate the quadratic models, further confirming the significant correlations between the independent variables and the observed responses. The best-fit regression model, which was established based on actual factors for the response parameter, was determined by Design-Expert as follows:

$$Decolorization\ rate\ (Y\%) = 0.3456 + 0.0682X_1 - 0.2627X_2 - 0.0125X_1X_2 + 0.0978{X_1}^2 + 0.1428{X_2}^2 \quad (2)$$

Table 2. The CCD design matrix for experimental design, observed and predicted response for MB removal.

Run	Voltage (kV)	pH	Decolorization rate%
1	30.5	6.5	28.1
2	28.0	9.0	36.4
3	33.0	9.0	43.0
4	34.0	6.5	61.1
5	30.5	6.5	40.2
6	27.0	6.5	36.2
7	30.5	6.5	32.9
8	30.5	6.5	33.5
9	33.0	4.0	94.5
10	28.0	4.0	81.6
11	30.5	10.0	18.1
12	30.5	6.5	37.5
13	30.5	3.0	97.9

Table 3 presents the results of the analysis of variance (ANOVA) that was used to test the significance of the developed models. With an F value of 29.59 and the corresponding p value of 0.0001, the model was considered significant according to the goodness-of-fit tests and there was a very low chance (0.02%) that the F value could occur due to noise. In addition, the insignificant lack of fit analysis results, with an F value of 4.27 and the corresponding p of 0.0972, indicated the adequacy of the model. The coefficients of determination (R^2) adjusted R^2 and predicted R^2 for decolorization rate were 0.9531, 0.9226, and 0.7384 respectively. The difference between adjusted R^2 and predicted R^2 is less than 0.2, meaning that the predicted R^2 is in reasonable agreement with the adjusted R^2. Besides, the linear correlations between the observed and predicted data for the decolorization rate were also obtained as shown in Figure 2a. The R^2 of 0.9531 implied that the model of decolorization rate has a high correction and could explain 95.31% of the total variation. Coefficients of variation for decolorization rate (14.68%) indicated clear agreement between the experimental and model results. Moreover, the adequate precision value (15.11, which measures the signal to noise ratio) for the model was larger than 4.0, indicating that the signals of the model were all adequate. In conclusion, all these statistical results showed that the developed model was able to predict the experimental data and adequately describe the relationship between the variables and

Preprints (www.preprints.org) | NOT PEER-REVIEWED | Posted: 11 December 2023 doi:10.20944/preprints202312.0738.v1

responses. To be more specific, this quadratic model was validated for describing the decolorization rate under different pH and voltage within the range used in this study.

Table 3. Analysis of variance (ANOVA) results for model terms.

Source	Sum of Squares	df	Mean Square	F-value	p-value	
Model	0.7750	5	0.1550	29.59	0.0001	significant
X_1-Voltage	0.0368	1	0.0368	7.03	0.0329	
X_2-pH	0.5520	1	0.5520	105.37	< 0.0001	
$X_1 X_2$	0.0006	1	0.0006	0.12	0.7399	
X_1^2	0.0646	1	0.0646	12.33	0.0098	
X_2^2	0.1421	1	0.1421	27.13	0.0012	
Residual	0.0367	7	0.0052			
Lack of Fit	0.0280	3	0.0093	4.27	0.0972	not significant
Pure Error	0.0087	4	0.0022			
Cor Total	0.8117	12				

R^2, 0.9531; adjusted R^2, 0.9226; predict R^2, 0.7384; adequate precision, 15.11; CV%, 14.68; standard deviation, 0.0724; Predicted Residual Error Sum of Squares (PRESS), 0.2124.

Figure 2b presents a surface response plot illustrating the decolorization rate as a function of pH and voltage. These plots are instrumental in determining the optimal conditions for the response variable within the selected experimental ranges. Analysis reveals that the maximal decolorization efficiency, quantified at 94.0%, was achieved at an optimal pH of 4 and a voltage of 33 kV. The figure clearly showed a substantial enhancement in the decolorization rate with increasing voltage, underscoring its pivotal role in plasma treatment. Furthermore, comparing experimental runs 6 and 9 in Table 2 indicated that the decolorization rate improved from 36% to 61% with a voltage increment from 27 kV to 33 kV. This phenomenon is attributable to the increased electric field intensity between the electrode and the solution surface, which significantly intensifies the formation of active species within the plasma streamers, thus facilitating their diffusion into the liquid phase.

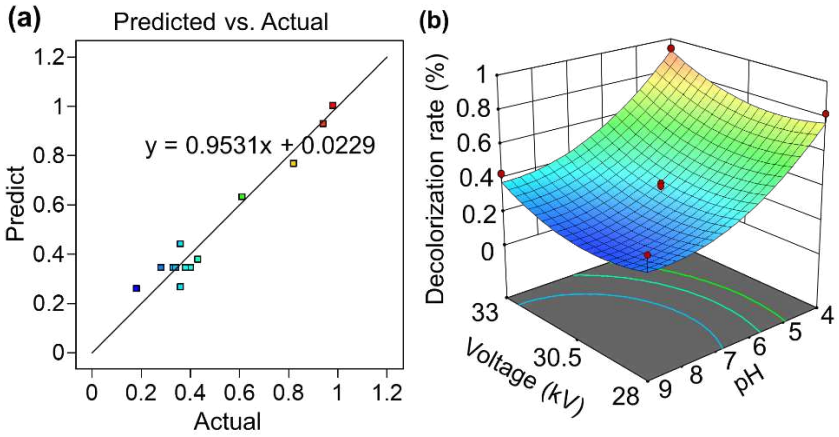

Figure 2. (a) Linear correlations between the observed and predicted data for decolorization rate, and (b) response surface plots of decolorization rate with respect to voltage and pH.

Equation 3 presents a coefficient of -0.2627 for the pH term, signifying a substantial inverse relationship with the degradation rate. Such a coefficient suggests that an acidic environment enhances the rate of degradation more effectively than neutral or alkaline conditions. This correlation is also graphically illustrated in Figure 2b. MB degradation was lower than 40% at a solution pH of 9, and it was increased to 94% at a solution pH of 4.

Preprints (www.preprints.org) | NOT PEER-REVIEWED | Posted: 11 December 2023 doi:10.20944/preprints202312.0738.v1

The enhanced degradation capability with decreasing pH is primarily due to the following reasons. First, the pH of the solution critically impacts the ionization potential of target pollutants, thereby affecting their reactivity and degradation. In aqueous environments, MB predominantly exists in its cationic form (MB^+). Under acidic conditions, MB transitions into a protonated form (MBH^{2+}), which alters its electronic structure. The increased protonation of the dimethylamino groups in acidic media enhances the susceptibility of the methyl groups to dissociation [14]. This protonation potentially facilitates the oxidative degradation of MB, making acidic conditions more conducive to its breakdown. Second, the detrimental impact of the hydroxyl anion (OH^-) in alkaline conditions may interfere with the effective reaction of the hydroxyl radical (·OH) [15]. In addition, the decomposition of hydrogen peroxide (H_2O_2) leads to the formation of hydroperoxide anion (HO_2^-), which can act as a quenching agent for ·OH [16]. It is important to note that the superoxide anion (O_2^-) generated in Equation 5 is a relatively weak nucleophile and reducing agent, which can reduce MB to a colorless reduced form but cannot decompose the MB molecules.

$$\cdot OH + OH^- \rightarrow O_2^{-\cdot} + H_2 \quad (3)$$

$$H_2O_2 \leftrightarrow HO_2^- + H^+ \quad (4)$$

$$HO_2^- + \cdot OH \rightarrow HO_2 + O_2^{-\cdot} \quad (5)$$

Moreover, the equilibrium between H_2O_2 and ·OH is pH-dependent, being more favorable in acidic solutions. The electrons generated by plasma can interact with water to produce hydrogen radicals (·H), which can react with oxygen to form hydroperoxyl radicals ($\cdot HO_2$) and superoxide anion radical ($O_2^{-\cdot}$) intermediates (Equation 6-7) [17]. These intermediates can enhance the generation of H_2O_2 production (Equations 8–10) [18]. Furthermore, in acidic conditions, H_2O_2 can decompose into ·OH (Equations 11), which possesses an exceptionally high oxidative potential (E_o) and ranking as the most potent among available oxidizing agents (only surpassed by fluorine). Thus, it can be concluded that a reduction in pH significantly enhances the degradation efficiency of MB.

$$H\cdot + O_2 \rightarrow HO_2\cdot \quad (6)$$

$$HO_2\cdot \xleftrightarrow{pka = 4.8} H^+ + O_2^{-\cdot} \quad (7)$$

$$HO_2\cdot + H^+ + O_2^{-\cdot} \rightarrow H_2O_2 + O_2 \quad (8)$$

$$HO_2\cdot + H^+ + e^- \rightarrow H_2O_2 \quad (9)$$

$$O_2 \xrightarrow{e^-} O_2^{-\cdot} \xrightarrow{e^-,2H^+} H_2O_2 \quad (10)$$

$$H_2O_2 \xrightarrow{e^-,2H^+} \cdot OH + H_2O \quad (11)$$

3.2. Reaction order and kinetics

The degradation of organic compounds in aqueous solutions through plasma treatment is predominantly characterized by first-order kinetics. If the degradation of MB aligns with the pseudo-first-order reaction model, the experimental data can be suitably fitted to the corresponding first-order kinetic Equation.

$$In(\frac{C}{C_0}) = k_0 * t \quad (12)$$

where $\boldsymbol{k_0}$ is the observed rate constant, C_0 and C are the initial dye concentration and the concentration after time t, respectively. Figure 3 presents the pseudo-first-order kinetic plot, demonstrating a linear relationship of $In(C/C_0)$ over time obtained at a pH of 3 and a voltage of 31.5 kV. The plot reveals a high correlation coefficient (R^2) of 0.9858 for the degradation process. This value indicates that the decomposition of MB aligns well with the characteristics of a pseudo-first-order reaction.

Preprints (www.preprints.org) | NOT PEER-REVIEWED | Posted: 11 December 2023 doi:10.20944/preprints202312.0738.v1

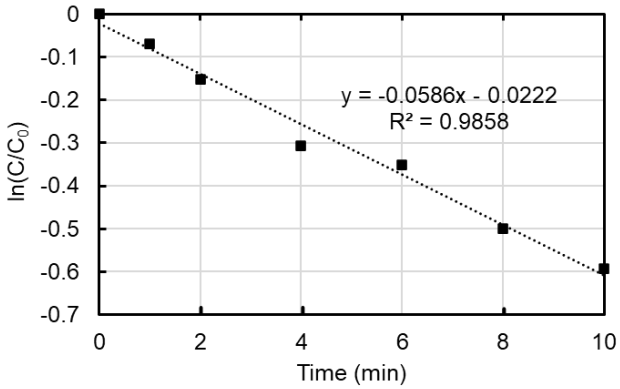

Figure 3. First-order linear plot of $\ln(C/C_0)$ versus time of MB degradation by non-thermal plasma.

3.3. Mechanism analysis

Wastewater treatment through plasma-induced reactions is facilitated by three distinct methods, each influencing the design of the reactors used [19]. The direct discharge approach involves immersing electrodes in water, creating a filamentary streamer discharge at high electric fields (around 1 MV/cm), which generates reactive oxygen species and produces OH radicals, hydrogen, and hydrogen peroxide. This method also induces shockwaves and UV radiation, aiding in the decomposition of organic contaminants and microorganisms. An alternative, the indirect discharge approach, generates plasma above the water surface, relying on the diffusion of plasma-produced species into the water, a process governed by Henry's law and requiring lower initiation voltage. Lastly, the bubbling method introduces plasma within injected bubbles in the water, effectively increasing the contact surface area between plasma and liquid and allowing for tailored chemical reactions, illustrating the diverse methodologies underlying plasma water purification systems. In this study, the indirect discharge method was used, since the gas phase plasma was more energy efficient [20].

In this indirect discharge process, plasma is generated between the anode tip and the water surface, forming a bright streamer discharge. This plasma interacts with the water surface, causing slight movements or small ripples due to the electro-hydrodynamic effect, which leads to surface deformation [21]. The primary mechanism for degrading pollutants in water through non-thermal plasma involves the production of a variety of reactive species after the collisions between accelerating electrons and neutrals. Primary reactive species with fleeting lifespans (1-3 μs) are formed in the gas phase immediately after the collision, including ionized neutrals and gas (M^+), excited neutrals and gas (M^*), N, O, atomic H, NO, and O_2^{*-} [22–24]. Then, some reactive species generated in the plasma process are subject to immediate radiative decay, while others would react with additional reactive species, neutral molecules, and water to form secondary reactive species like hydrogen peroxide (H_2O_2), nitrogen dioxide (NO_2), nitric oxide (NO), and ozone (O_3) in the surrounding air [25,26]. These secondary reactive species, once generated in the gas phase, would migrate into the liquid phase or other substrates, where the formed tertiary reactive species expand their lifetimes from milliseconds to several days. Tertiary reactive species are more stable, including O_3, H_2O_2, nitrate (NO_3^-), peroxynitrite ($ONOO^-$), and nitrite (NO_2^-). Figure 4 visually summarizes the reactive species formation process from the discharge region through the gas phase to the target substrate.

Preprints (www.preprints.org) | NOT PEER-REVIEWED | Posted: 11 December 2023 doi:10.20944/preprints202312.0738.v1

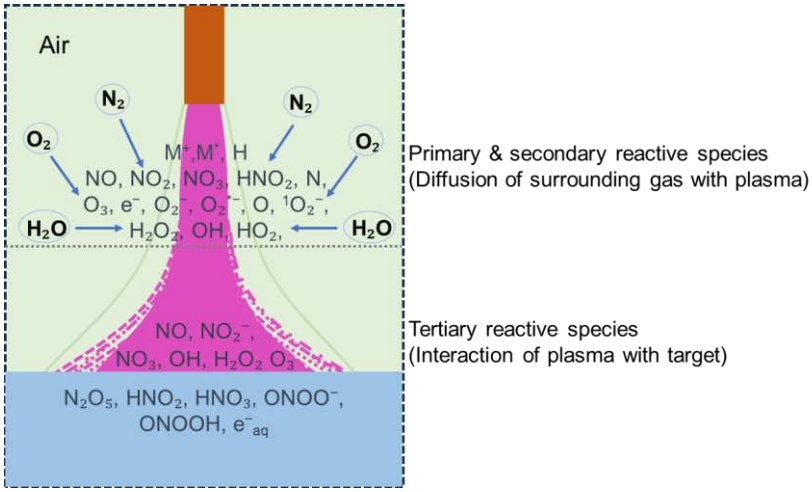

Figure 4. Schematic diagram representing the formation of various reactive species in the non-thermal atmospheric pressure plasma.

In the plasma-treated substrate, the electrolytic dissociation of water is also facilitated by plasma-generated electrons, yielding H_2O_2 through Equations 13-14. Hydrogen peroxide is a stable oxidizing agent formed not only via direct electron impact with water molecules but also through the dimerization of hydroxyl radicals. The in-situ generation of H_2O_2 serves as a proxy for the presence and reactivity of hydroxyl radicals within the plasma-mediated process [27]. Additionally, the peroxynitrous acid, a reactive nitrogenous intermediate, undergoes homolysis to yield ·NO and ·OH [28], which are integral to the oxidative degradation pathway.

$$H_2O^* + H_2O \rightarrow \cdot H + \cdot OH + H_2O \quad (13)$$

$$\cdot OH + \cdot OH \rightarrow H_2O_2 \quad (14)$$

The reactive species produced can engage in various mechanistic pathways when interacting with organic dye molecules. These pathways include electrophilic addition, hydrogen abstraction, and initiation of radical chain reactions. Photochemical dissociation by ultraviolet (UV) photons, as well as electron and ion-induced fragmentation, contributes to the multitudinous routes of MB molecular decomposition. UV can also dissociate hydrogen peroxide molecules present in aqueous solution to further improve the formation of highly reactive hydroxyl radicals [29]. This results in the disruption of conjugated chromophoric systems and the oxidative opening of aromatic ring structures, ultimately leading to the conversion into innocuous end-products like carbon dioxide and water.

$$H_2O_2 + h\nu \rightarrow 2 \cdot OH \quad (15)$$

The initial step of MB degradation is characterized by the homolytic cleavage of the N–CH_3 bond, which is the least energetically stable with a bond dissociation energy of 70.8 kcal/mol [3]. This process yields methyl radicals that are subsequently oxidized to methanol (CH_3OH), formic acid (HCOOH), or formaldehyde (HCHO). The carbon-sulfur (C–S) bond and carbon-nitrogen (C–N) bond are the most active parts of the remaining structure, which means they are more likely to be attacked by reactive radicals or ozone due to their lower bond dissociation energies compared to other molecular bonds present [30]. The degradation intermediates generated can undergo further oxidation reactions, leading either to complete mineralization or to the formation of less complex organic species, as shown in Figure 5.

Preprints (www.preprints.org) | NOT PEER-REVIEWED | Posted: 11 December 2023 doi:10.20944/preprints202312.0738.v1

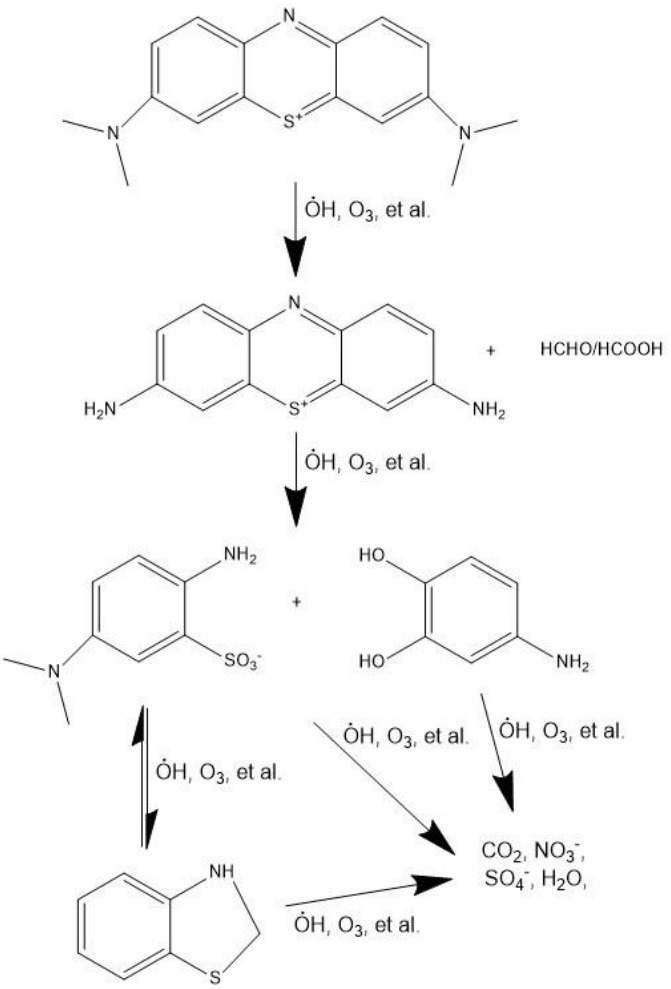

Figure 5. Proposed degradation mechanism pathway of methylene blue dye in cDBD system.

3.4. Practical analysis

Evaluating the efficiency of AOP in wastewater treatment is very important and often characterized by kinetic rate constants. However, these constants alone do not encompass other aspects of AOP efficiency, particularly the operational costs. To fill this gap, Bolton et al [31] introduced the Electrical Energy per Order (EE/O), defined by Equation (16). EE/O measures the electrical energy required per reactor volume to decrease a target contaminant's concentration by one order of magnitude, a critical metric in evaluating the energy consumption, which constitutes a significant portion of AOP operating costs. This metric is especially relevant for scenarios with low initial pollutant concentration (C_0) and is a critical measure of operational costs and instrumental in effectively scaling up treatment designs and estimating costs. The calculated EE/O value provides a benchmark for assessing the energy efficiency of the plasma treatment relative to other AOPs. A lower EE/O signifies greater energy efficiency and cost-effectiveness in contaminant reduction.

$$EE/O = \frac{P_{elec} * t * 1000}{V * 60 * \log(C_0/C)} \quad (16)$$

where P_{elec} is system power (kW), V is volume of water treated (L) in time t (min), C_0 is the initial contaminant concentration (EEO is valid for low initial concentrations, typically < 100 mg/L) and C is the final concentration [32].

For non-thermal plasma treatment process in this study, the total electrical energy utilized was 2.78 watts for treating a volume of 10 mL over 20 minutes, with a 50% duty cycle. The process successfully reduced the initial concentration of the contaminant from 20 ppm to 0.7 ppm. According to Equation (16), the EE/O = $(0.00278 * (20*50\%) * 1000)/(0.01 * 60 * \log(20/0.7)) = 31.82$ kWh/m^3/order for an initial concentration of 20 mg/L.

Preprints (www.preprints.org) | NOT PEER-REVIEWED | Posted: 11 December 2023 doi:10.20944/preprints202312.0738.v1

The plasma treatment system, requiring no oxidants, has a cost advantage over other AOPs and is competitive in the market. A brief economic comparison of different AOPs, such as ultrasonication (U/S), O_3, and UV treatments, is provided in Table 4. Notably, this moderate EE/O number is even lower than other existing efficient systems in low initial concentration.

Table 4. A comparison of plasma technologies with other AOPs employed for dye removal.

AOPs	C_0	C	Chemicals cost ($)	Energy density used (watt/ml)	EE/O (kWh/m³/order)	Total capital cost ($)	Reference
US	20	2	NA	0.50	10964.69	1.83E+10	[33,34]
O_3	20	2	NA	0.03	103.91	4.53E+05	[33,34]
U/S + UV	20	2	NA	0.53	3698.09	5.86E+09	[33,34]
U/S + O_3	20	2	NA	0.53	1215.02	1.92E+09	[33,34]
UV + O_3	20	2	NA	0.06	111.56	1.12E+07	[33,34]
U/S + UV + O_3	20	2	NA	0.56	989.9	1.50E+09	[33,34]
U/S + H_2O_2	100	45.65	2.06E+05	0.03	43.07	5.33E+08	[33,35]
UV + H_2O_2	100	84.35	2.06E+05	0.01	559.2	9.09E+07	[33,35]
U/S + UV + H_2O_2	100	9.13	2.06E+05	0.04	39.76	7.99E+07	[33,35]
Photocatalysis	402.6	40.26	2.52E+04	0.71	3654.68	2.67E+08	[33,36]
U/S + photocatalysis	402.6	40.26	6.98E+03	0.76	1059.08	1.11E+08	[33,36]
Plasma	20	0.7	NA	0.33	31.82	62	This study
Plasma	10	0.1	NA	0.15	5.79	62	This study

The comprehensive data from various AOPs, as summarized in Table 4, elucidate the relative economic and efficiency profiles of each method. The findings indicate that while standalone methods like U/S are cost-intensive, their integration with other AOPs can yield more economically viable solutions. For instance, U/S treatment alone exhibits a higher EE/O of 10964 kWh/m³/order, which significantly diminishes to 989 kWh/m³/order when combined with UV or O_3 treatments. This suggests that non-thermal plasma can also combine with other technologies to further enhance wastewater treatment efficiency.

The elevated total water treatment cost observed in this study is primarily attributed to the limited capacity of the employed reactor. Notably, the reactor operated without the introduction of any gases and featured a straightforward experimental setup, indicating substantial potential for future enhancements and optimization. Furthermore, the overall treatment efficiency could be further increased if the process was applied on a larger scale. Additionally, a study by Fahmy et al. [37] provided valuable insights into optimizing the removal of Acid Orange 142 dye. They achieved an 88.87% removal efficiency in treating 100 mL of wastewater with a 20 mg/L dye concentration, using a 12.5 kV voltage and a 5 mm gap between the solution surface and the high-voltage electrode over 90 minutes. Their energy consumption under these conditions was 2.025 kWh, equating to 30.375 W/mL. In contrast, our study recorded a substantially lower energy consumption rate of 0.33 W/mL, while achieving a higher decolorization rate of 96.5%, indicating a more efficient process for dye decolorization. These results clearly showed the effectiveness of this reactor.

In comparison to other AOPs utilized for water treatment, the efficiency and cost of the current plasma-based technology are quite competitive. These findings suggest that plasma technology not only holds broad application prospects but also, when integrated with other AOPs, can lead to further

cost reductions. The potential for cost-effective scalability and the ability to integrate seamlessly with other treatment methods make plasma technology a promising option in advancing sustainable water treatment strategies.

4. Conclusions

In conclusion, this study introduced an ultra-low cost cDBD plasma device, offering an affordable and efficient solution to wastewater treatment. The performance of the plasma discharger was optimized using CCD/RSM with the initial pH and applied voltage as independent variables. The prediction model had achieved a high correlation coefficient (R^2 = 0.9763) between the experimental data and the model's predictions. The research finding fills a crucial gap by analyzing the effects of initial pH and voltage on the degradation efficiency of organic pollutants and, specifically, by detailing the mechanisms of ROS generation and the degradation pathways of MB. The practical viability and efficiency of the plasma device to degrade MB were demonstrated by a low energy density and EE/O of 0.15 watt/mL and 5.79 kWh/m^3/order, respectively. This research not only demonstrates that plasma is a promising and environmental-friendly option for dye wastewater treatment, but also establishes a foundation for ongoing innovation in non-thermal plasma applications.

Author Contributions: Conceptualization, Y.X. and Y.T.; methodology, Y.X. and Y.T.; software, Y.X.; validation, Y.X. and Y.T.; formal analysis, Y.X.; investigation, Y.X and Y.T.; resources, J.Z and Y.Z.; data curation, Y.T.; writing—original draft preparation, Y.X. and Y.T.; writing—review and editing, J.Z., Y.X., Y.T, and Y.Z.; visualization, Y.X.; supervision, J.Z.; project administration, J.Z; funding acquisition, J.Z. All authors have read and agreed to the published version of the manuscript.

Data Availability Statement: All data is available upon reasonable request.

Acknowledgments: This research was supported by the Arkansas Agriculture Experiment Station of the University of Arkansas Division of Agriculture and the Center for Agricultural and Rural Sustainability.

Conflicts of Interest: The authors declare no conflict of interest.

References

1. A, V.A. Environmental Pollution during Chemical Processing of Synthetic Fibers. *Colourage* **1982**, *14*, 3–10.
2. Chung, K.-T.; Stevens Jr., S.E. Degradation Azo Dyes by Environmental Microorganisms and Helminths. *Environmental Toxicology and Chemistry* **1993**, *12*, 2121–2132, doi:10.1002/etc.5620121120.
3. Khan, I.; Saeed, K.; Zekker, I.; Zhang, B.; Hendi, A.H.; Ahmad, A.; Ahmad, S.; Zada, N.; Ahmad, H.; Shah, L.A.; et al. Review on Methylene Blue: Its Properties, Uses, Toxicity and Photodegradation. *Water* **2022**, *14*, 242, doi:10.3390/w14020242.
4. Krishna Moorthy, A.; Govindarajan Rathi, B.; Shukla, S.P.; Kumar, K.; Shree Bharti, V. Acute Toxicity of Textile Dye Methylene Blue on Growth and Metabolism of Selected Freshwater Microalgae. *Environmental Toxicology and Pharmacology* **2021**, *82*, 103552, doi:10.1016/j.etap.2020.103552.
5. Rashid, R.; Shafiq, I.; Akhter, P.; Iqbal, M.J.; Hussain, M. A State-of-the-Art Review on Wastewater Treatment Techniques: The Effectiveness of Adsorption Method. *Environ Sci Pollut Res* **2021**, *28*, 9050–9066, doi:10.1007/s11356-021-12395-x.
6. Zhang, Y.; Cai, J.; Dan, Z.; Tian, Y.; Duan, N.; Xin, B. Simultaneous Oxidative Degradation of Toxic Acid Wastewater from Production of Nitrocellulose and Release of Mn2+ from Low-Grade MnO2 Ore as Oxidant. *Journal of Chemical Technology & Biotechnology* **2017**, *92*, 1638–1644, doi:10.1002/jctb.5159.
7. Xiao, Y.; Tian, Y.; Zhan, Y.; Zhu, J. DEGRADATION OF ORGANIC POLLUTANTS IN FLOCCULATED LIQUID DIGESTATE USING PHOTOCATALYTIC TITANATE NANOFIBERS: MECHANISM AND RESPONSE SURFACE OPTIMIZATION. *Front. Agr. Sci. Eng.* **2023**, 0, doi:10.15302/J-FASE-2023503.
8. Deng, Y.; Zhao, R. Advanced Oxidation Processes (AOPs) in Wastewater Treatment. *Curr Pollution Rep* **2015**, *1*, 167–176, doi:10.1007/s40726-015-0015-z.
9. Rayaroth, M.P.; Aravindakumar, C.T.; Shah, N.S.; Boczkaj, G. Advanced Oxidation Processes (AOPs) Based Wastewater Treatment - Unexpected Nitration Side Reactions - a Serious Environmental Issue: A Review. *Chemical Engineering Journal* **2022**, *430*, 133002, doi:10.1016/j.cej.2021.133002.

10. Epelle, E.I.; Macfarlane, A.; Cusack, M.; Burns, A.; Okolie, J.A.; Vichare, P.; Rolland, L.; Yaseen, M. Ozone Decontamination of Medical and Nonmedical Devices: An Assessment of Design and Implementation Considerations. *Ind Eng Chem Res* **2023**, *62*, 4191–4209, doi:10.1021/acs.iecr.2c03754.
11. Peroxone: Ozone Peroxide Advanced Oxidation Processes AOP. *Spartan Water Treatment*.
12. He, Y.; Sang, W.; Lu, W.; Zhang, W.; Zhan, C.; Jia, D. Recent Advances of Emerging Organic Pollutants Degradation in Environment by Non-Thermal Plasma Technology: A Review. *Water* **2022**, *14*, 1351, doi:10.3390/w14091351.
13. Gururani, P.; Bhatnagar, P.; Bisht, B.; Kumar, V.; Joshi, N.C.; Tomar, M.S.; Pathak, B. Cold Plasma Technology: Advanced and Sustainable Approach for Wastewater Treatment. *Environ Sci Pollut Res Int* **2021**, *28*, 65062–65082, doi:10.1007/s11356-021-16741-x.
14. Minamoto, C.; Fujiwara, N.; Shigekawa, Y.; Tada, K.; Yano, J.; Yokoyama, T.; Minamoto, Y.; Nakayama, S. Effect of Acidic Conditions on Decomposition of Methylene Blue in Aqueous Solution by Air Microbubbles. *Chemosphere* **2021**, *263*, 128141, doi:10.1016/j.chemosphere.2020.128141.
15. Zheng, K.; Sun, Y.; Gong, S.; Jiang, G.; Zheng, X.; Yu, Z. Degradation of Sulfamethoxazole in Aqueous Solution by Dielectric Barrier Discharge Plasma Combined with Bi2WO6 -RMoS2 Nanocomposite: Mechanism and Degradation Pathway. *Chemosphere* **2019**, *222*, 872–883, doi:10.1016/j.chemosphere.2019.02.004.
16. Guan, R.; Yuan, X.; Wu, Z.; Jiang, L.; Li, Y.; Zeng, G. Principle and Application of Hydrogen Peroxide Based Advanced Oxidation Processes in Activated Sludge Treatment: A Review. *Chemical Engineering Journal* **2018**, *339*, 519–530, doi:10.1016/j.cej.2018.01.153.
17. Ahmadi, E.; Shokri, B.; Mesdaghinia, A.; Nabizadeh, R.; Reza Khani, M.; Yousefzadeh, S.; Salehi, M.; Yaghmaeian, K. Synergistic Effects of α-Fe2O3-TiO2 and Na2S2O8 on the Performance of a Non-Thermal Plasma Reactor as a Novel Catalytic Oxidation Process for Dimethyl Phthalate Degradation. *Separation and Purification Technology* **2020**, *250*, 117185, doi:10.1016/j.seppur.2020.117185.
18. Wang, T.; Qu, G.; Sun, Q.; Liang, D.; Hu, S. Evaluation of the Potential of P-Nitrophenol Degradation in Dredged Sediment by Pulsed Discharge Plasma. *Water Research* **2015**, *84*, 18–24, doi:10.1016/j.watres.2015.07.022.
19. Locke, B.R.; Sato, M.; Sunka, P.; Hoffmann, M.R.; Chang, J.-S. Electrohydraulic Discharge and Nonthermal Plasma for Water Treatment. *Ind. Eng. Chem. Res.* **2006**, *45*, 882–905, doi:10.1021/ie050981u.
20. Foster, J.E. Plasma-Based Water Purification: Challenges and Prospects for the Future. *Physics of Plasmas* **2017**, *24*, 055501, doi:10.1063/1.4977921.
21. Kim, H.H.; Teramoto, Y.; Negishi, N.; Ogata, A.; Kim, J.H.; Pongrác, B.; Machala, Z.; Gañán-Calvo, A.M. Polarity Effect on the Electrohydrodynamic (EHD) Spray of Water. *Journal of Aerosol Science* **2014**, *76*, 98–114, doi:10.1016/j.jaerosci.2014.06.002.
22. Lim, J.S.; Kim, R.H.; Hong, Y.J.; Lamichhane, P.; Adhikari, B.C.; Choi, J.; Choi, E.H. Interactions between Atmospheric Pressure Plasma Jet and Deionized Water Surface. *Results in Physics* **2020**, *19*, 103569, doi:10.1016/j.rinp.2020.103569.
23. Lamichhane, P.; Paneru, R.; N. Nguyen, L.; Sup Lim, J.; Bhartiya, P.; Chandra Adhikari, B.; Mumtaz, S.; Ha Choi, E. Plasma-Assisted Nitrogen Fixation in Water with Various Metals. *Reaction Chemistry & Engineering* **2020**, *5*, 2053–2057, doi:10.1039/D0RE00248H.
24. Attri, P.; Kim, Y.H.; Park, D.H.; Park, J.H.; Hong, Y.J.; Uhm, H.S.; Kim, K.-N.; Fridman, A.; Choi, E.H. Generation Mechanism of Hydroxyl Radical Species and Its Lifetime Prediction during the Plasma-Initiated Ultraviolet (UV) Photolysis. *Sci Rep* **2015**, *5*, 9332, doi:10.1038/srep09332.
25. Ghimire, B.; Lamichhane, P.; Lim, J.S.; Min, B.; Paneru, R.; Weltmann, K.-D.; Choi, E.H. An Atmospheric Pressure Plasma Jet Operated by Injecting Natural Air. *Applied Physics Letters* **2018**, *113*, 194101, doi:10.1063/1.5055592.
26. Barjasteh, A.; Dehghani, Z.; Lamichhane, P.; Kaushik, N.; Choi, E.H.; Kaushik, N.K. Recent Progress in Applications of Non-Thermal Plasma for Water Purification, Bio-Sterilization, and Decontamination. *Applied Sciences* **2021**, *11*, 3372, doi:10.3390/app11083372.
27. Palma, D.; Richard, C.; Minella, M. State of the Art and Perspectives about Non-Thermal Plasma Applications for the Removal of PFAS in Water. *Chemical Engineering Journal Advances* **2022**, *10*, 100253, doi:10.1016/j.ceja.2022.100253.
28. Merényi, G.; Lind, J. Free Radical Formation in the Peroxynitrous Acid (ONOOH)/Peroxynitrite (ONOO-) System. *Chem Res Toxicol* **1998**, *11*, 243–246, doi:10.1021/tx980026s.

29. Manoj Kumar Reddy, P.; Rama Raju, B.; Karuppiah, J.; Linga Reddy, E.; Subrahmanyam, Ch. Degradation and Mineralization of Methylene Blue by Dielectric Barrier Discharge Non-Thermal Plasma Reactor. *Chemical Engineering Journal* **2013**, *217*, 41–47, doi:10.1016/j.cej.2012.11.116.
30. Huang, F.; Chen, L.; Wang, H.; Yan, Z. Analysis of the Degradation Mechanism of Methylene Blue by Atmospheric Pressure Dielectric Barrier Discharge Plasma. *Chemical Engineering Journal* **2010**, *162*, 250–256, doi:10.1016/j.cej.2010.05.041.
31. Bolton, J.R.; Bircher, K.G.; Tumas, W.; Tolman, C.A. Figures-of-Merit for the Technical Development and Application of Advanced Oxidation Technologies for Both Electric- and Solar-Driven Systems (IUPAC Technical Report). *Pure and Applied Chemistry* **2001**, *73*, 627–637, doi:10.1351/pac200173040627.
32. Advanced Oxidation Processes—With so Many Options, How Can We Gauge Efficiency? Available online: https://wcponline.com/2021/08/15/advanced-oxidation-processes-with-so-many-options-how-can-we-gauge-efficiency/ (accessed on 8 December 2023).
33. Mahamuni, N.N.; Adewuyi, Y.G. Advanced Oxidation Processes (AOPs) Involving Ultrasound for Waste Water Treatment: A Review with Emphasis on Cost Estimation. *Ultrasonics Sonochemistry* **2010**, *17*, 990–1003, doi:10.1016/j.ultsonch.2009.09.005.
34. Tezcanli-Güyer, G.; Ince, N.H. Individual and Combined Effects of Ultrasound, Ozone and UV Irradiation: A Case Study with Textile Dyes. *Ultrasonics* **2004**, *42*, 603–609, doi:10.1016/j.ultras.2004.01.096.
35. Fung, P.C.; Sin, K.M.; Tsui, S.M. Decolorisation and Degradation Kinetics of Reactive Dye Wastewater by a UV/Ultrasonic/Peroxide System. *Coloration Technology* **2000**, *116*, 170–173, doi:10.1111/j.1478-4408.2000.tb00036.x.
36. An, T.; Gu, H.; Xiong, Y.; Chen, W.; Zhu, X.; Sheng, G.; Fu, J. Decolourization and COD Removal from Reactive Dye-Containing Wastewater Using Sonophotocatalytic Technology. *Journal of Chemical Technology & Biotechnology* **2003**, *78*, 1142–1148, doi:10.1002/jctb.915.
37. Fahmy, A.; El-Zomrawy, A.; Saeed, A.M.; Sayed, A.Z.; El-Arab, M.A.E.; Shehata, H.; Friedrich, J. Degradation of Organic Dye Using Plasma Discharge: Optimization, PH and Energy. *Plasma Res. Express* **2020**, *2*, 015009, doi:10.1088/2516-1067/ab6703.